

# Analysis of Pulsating Components in the Eclipsing Binary Systems LT Herculis, RZ Microscopii, LY Puppis, V632 Scorpii, and V638 Scorpii

**Margaret Streamer**

*Variable Stars South; 3 Lupin Place, Murrumbateman, NSW 2582, Australia; m.stream@bigpond.com*

**Terry Bohlsen**

*Variable Stars South; Mirranook, Armidale, NSW 2350, Australia*

**Yenal Ogmen**

*Variable Stars South; P.O. Box 756, Nicosia, North Cyprus via Mersin 10, Turkey*

*Received March 7, 2016; revised April 12, 2016; accepted April 20, 2016*

**Abstract** Eclipsing binary stars are especially valuable for studies of stellar evolution. If pulsating components are also present then the stellar interior can be studied using asteroseismology techniques. We present photometric data and the analysis of the  $\delta$  Scuti pulsations that we have discovered in five eclipsing binary systems. The systems are: LT Herculis, RZ Microscopii, LY Puppis, V632 Scorpii, and V638 Scorpii. The dominant pulsation frequencies range from 13 to 29 cycles per day with semi-amplitudes of 4 to 20 millimagnitudes.

## 1. Introduction

Members of Variable Stars South have discovered seven systems with pulsating components found while obtaining accurate eclipse timings to update light elements of poorly studied southern eclipsing binaries (Moriarty *et al.* 2013; Streamer *et al.* 2015). We have previously reported the pulsation properties of three of these binary systems (Moriarty *et al.* 2013). Here we report the pulsation properties of four more of these binaries and include an eighth, newly discovered system, LY Puppis.

The evolutionary history of pulsating stars, in this case  $\delta$  Scuti type, in a binary system is considerably different from those of isolated  $\delta$  Scuti stars, making the former valuable for investigations of the stellar interior and other astrophysical properties of this type of star.

Ground-based astronomers, at best, can only obtain uninterrupted portions of light curves of eclipsing binary systems spanning entire nights. A team of observers in different longitudes can provide better coverage but all are constrained by cloud, full moon, changes in air mass, poor seeing and/or transparency and the unavoidable day/night and seasonal cycles. Nevertheless, high frequency pulsations, such as the  $\delta$  Scuti type, are readily detected in high-cadence data sets.

Fourier analysis of the individual light curves reveals the frequency and amplitude of the pulsations which in turn gives information about the stellar interior. However, analysis of such short duration observations, in which only a few pulsation cycles are observed, must be considered cautiously. Also, cycle count

ambiguities are present if data sets from consecutive nights are combined and sampled (see Murphy (2015) for a review of aliasing in the context of Fourier analysis of  $\delta$  Scuti stars). At best, only one or two frequencies are reliably identified from short-duration data. In contrast, space-based instrumentation, such as the Kepler Mission, provides data of high precision, long duration, and continuity. Fourier analysis of Kepler data typically reveals multiple frequencies. For example, Hambleton *et al.* (2013) identified 32 frequencies in the binary KIC 4544587.

Fourier analysis of the pulsations we observed gives frequencies and amplitudes of the dominant pulsations confirming the  $\delta$  Scuti component of the systems studied. LT Her has previously been reported to have a  $\delta$  Scuti component by Liakos and Niarchos (2015) but none of the other of our targets are listed in their catalogue.

## 2. Observations and analysis

Time series photometry was performed with the instruments given in Table 1. Each observer used NTP software such as DIMENSION 4 (Thinking Man Software 1992–2014) to synchronize their computer's clock to UTC. A fast cadence was used to acquire the photometric data to ensure good coverage of the pulsations and for accurate determination of the eclipse times of minima. Typical exposure times were of 60 to 120 seconds with delays between each exposure (for image download) of about 30 seconds. Targets were also observed during secondary eclipses and out of eclipse for the longest duration possible in

Table 1. Photometric equipment used by the authors.

Observer	Initials	Telescope	Camera
Streamer	MS	350-mm Meade Schmidt-Cassegrain	SBIG ST8XME CCD
Ogmen	YO	356-mm Meade LX200R (ACF)	SBIG ST8XME CCD
Bohlsen	TB	200-mm Vixen VC200L Cassegrain	SBIG ST10XME CCD

any one night to maximize the time span available for Fourier analysis of the pulsations.

Most CCD imaging was done with Johnson V filters; some data for LT Her were also obtained with a clear filter. The images were reduced using aperture photometry; details of the comparison stars are given in Table 2. The resulting magnitude data are untransformed. Details of the observation logs are also given in Table 2 along with the spectral classification of each system as reported in the literature.

Times of minima were determined using the Polynomial fit in PERANSO (Vanmunster 2013). Pulsation frequencies were analysed using Fourier methods in PERIOD04 (Lenz and Breger 2005), using as many data sets as possible for each target. For analysis of pulsations in secondary eclipses, a polynomial fit to the eclipse curve was first subtracted.

Additionally, Bohlsen determined the spectral type of V632 Sco from a spectrum obtained with a LISA spectrograph on a Celestron C11 SCT using an Atik 314L+ CCD with a resolution of  $R = 1000$  and a S/N of approximately 100. The spectrum was calibrated using a neon calibration light.

The spectrum was compared to known standards in the MK Spectral classification system, with a resolution of 3.6 Angstrom, from the Dark Sky Observatory at the Appalachian State University (Gray 2013). The accuracy of the spectral classification was limited by the resolution and the S/N of equipment.

### 3. Results and Discussion

Updated light elements for RZ Mic, V632 Sco, and V638 Sco were previously reported by Streamer *et al.* (2015). Regression analysis of three primary minima for LT Her give a current epoch (HJD) of  $2455752.3219 \pm 0.0028$  and a period of  $1.0840 \pm 0.0001$  days. Only one complete primary eclipse has been observed for LY Pup, giving an improved epoch of  $2456695.1274 \pm 0.0027$  HJD using the period of  $2.8879 \pm 0.0001$  days from the *General Catalogue of Variable Stars* (GCVS; Kholopov *et al.* 1985) as reference.

Results of the Fourier analysis of the pulsations for each target are given in Table 3 with examples of power spectra given in Figure 1. Examples of primary and secondary eclipses, as well as uneclipsed portions of the orbital cycle, for each target are shown in Figures 2 through 15.

#### 3.1. RZ Microscopii

RZ Mic (V mag. = 11.35, P = 3.9830 days) has a 0.95-magnitude primary eclipse and a 0.25-magnitude secondary eclipse. The primary eclipse is about 0.5 magnitude deeper than reported in the International Variable Star Index (VSX; Watson *et al.* 2014) but our results agree with ASAS observations (Pojmański 1997). Of all the targets reported here, RZ Mic has the highest-amplitude  $\delta$  Scuti pulsations. The pulsations are evident during all orbital phases (Figures 2, 3, and 4) although during the primary eclipse (Figure 2) they only appear as distortions on the otherwise smooth curve. Two pulsation frequencies were identified, with the dominant frequency being  $13.52 \pm 0.04$  cycles/day with a semi-amplitude of  $19 \pm 0.6$  millimagnitudes (Table 3). A much lower amplitude ( $4 \pm 0.7$  mmag.) second frequency ( $25.67 \pm 0.20$  c/d) was also consistently extracted from the individual data sets. The same frequencies were confirmed when observations from four consecutive nights were combined and analyzed.

#### 3.2. LY Puppis

LY Pup (V mag. = 12.35, P = 2.8879 days) has eclipses of over 9 hours duration. Thus, observing complete eclipses during the short summer nights when the target is visible in Australia is difficult. However, one complete primary eclipse of 0.85 magnitude was obtained and is shown in Figure 5. Pulsations are hardly evident in this eclipse although they are seen in other incomplete primary eclipses. One of these is also shown in Figure 5. In contrast, pulsations are easily detected during the small secondary eclipse of 0.03 magnitude (Figure 6) and in uneclipsed portions of the light curve (Figure 7). Two pulsation frequencies were extracted: a primary frequency of  $27.15 \pm 0.13$  c/d with a semi-amplitude of  $20 \pm 1$  mmag. and a slightly lower one of  $25.45 \pm 0.48$  c/d with an amplitude approximately half that of F1 ( $9 \pm 1$  mmag.). The two light curves (Figures 6 and 7) clearly show these amplitude differences. The high amplitude, primary frequency, F1, has only been observed twice out of the six data sets analyzed. The short time-span of each data set, coupled with the similarity of the two extracted frequencies, suggests the addition/interference of each frequency component creates a beat pattern which obscures the high-amplitude frequency. Examples of the power spectra for the data sets exhibiting the two different frequencies are shown in Figure 1.

Table 2. Comparison stars and their magnitudes, observation logs and spectral type of each binary system.

Binary System	Comparison Star	V Mag. Comp.	Number of Nights Observed	Number of Hours Observed	Phase Observed	Spectral Type
LT Her	GSC 0966 1191	9.774	7	27	0.0–0.25,	A2V+[F3] <sup>1</sup>
	GSC 0966 1345	11.07			0.35–0.6, 0.8–1.0	A2V <sup>2</sup>
RZ Mic	GSC 7972 0135	11.310	19	174	0.0–1.0	A5+[F4.5] <sup>1</sup>
LY Pup	GSC 6555 0556	10.568	12	71.5	0.0–1.0	(A5)+[K0IV] <sup>1</sup>
V632 Sco	GSC 7891 0318	11.551	10	48.5	0.0–0.24,	F2 + [K4–K5] <sup>3</sup>
	GSC 7891 0006	10.929			0.37–1.0	F0V or F1V <sup>4</sup>
V638 Sco	GSC 7891 0378	11.110	13	81.4	0.4–1.0	A(8)+[G8IV] <sup>1</sup>

Notes: 1—Spectral types from Svehnikov and Kuznetsova (1990); 2—Spectral type from Ebbighausen and Penegor (1974); 3—Spectral type from Giuricin *et al.* (1984); 4—Bohlsen, this work.

Table 3. Dominant frequencies with their semi-amplitudes for each target.

<i>Binary System</i>	<i>Pulsation F1 (cycles/day)</i>	<i>Pulsation F2 (cycles/day)</i>	<i>Pulsation Amp 1 (millimag.)</i>	<i>Pulsation Amp 2 (millimag.)</i>
LT Her	28.87±0.09		6±1	
RZ Mic	13.52±0.04	25.67±0.20	19±0.6	4±0.7
LY Pup	27.15±0.13	25.45±0.48	20±1	9±1
V632 Sco	25.58±0.10		6±1	
V638 Sco	15.23±0.23		5±1	

### 3.3. LT Herculis, V632 Scorpii, and V638 Scorpii

LT Her, V632 Sco, and V638 Sco are all characterized by low amplitude pulsations from 4 to 6 mmag. Only one pulsation frequency was reliably extracted from the data for each target. Even though the three targets are not particularly dim, the pulsation amplitudes are small and approaching the limits of detection for our equipment. Good photometric conditions were needed to reliably record the pulsations. However, we are confident of the existence of pulsations in these target systems as they have been recorded numerous times and independently by members of our group.

The data for LT Her (V mag. = 10.5, P = 1.0840 days) were collected using different comparison stars with either no filter or a V filter. For easier comparison, Figures 8 and 9 are given as  $\Delta$  magnitudes rather than as untransformed magnitudes. A primary eclipse (Figure 8) shows the distortions imposed upon the light curve by the pulsations of the primary component and Figure 9 shows the pulsations clearly at the end of an eclipse. The single frequency extracted ( $28.87 \pm 0.09$  c/d) has a semi-amplitude of  $6 \pm 1$  mmag. Liakos and Niarchos (2015) have also reported a primary frequency of 30.800c/d which differs slightly from what we determined. The latter did not report errors or the amplitude of this frequency, so it is difficult to establish if the differences are real.

Earlier studies of LT Her by Ebbighausen and Penegor (1974) clearly show pulsations, although they interpreted the effect to be due to gas transfer between the component stars.

Data reduction of observations of V632 Sco (V mag. = 11.2, P = 1.6102 days) is hampered by the close proximity of other stars which are not completely resolved during poor seeing conditions. However, after numerous observations by three different observers, we are confident that a pulsating component is present in the binary system (Figures 10, 11, and 12). A dominant frequency of  $25.63 \pm 0.14$  c/d with semi-amplitude  $6 \pm 1$  mmag. was extracted from the data sets.

Our spectral classification for V632 Sco is F0V or F1V, suggesting that the primary component is hotter than that given by Giuricin *et al.* (1984) who determined the spectral classification for the system as F2 + [K4-K5].

The pulsations in V638 Sco (V mag. = 10.8, P = 2.3583 days) have the lowest amplitude of all the targets reported in this paper. Excellent photometric conditions are needed to see the pulsations which have a semi-amplitude of only  $4 \pm 1$  mmag. Figure 13 shows a primary eclipse which is distorted by the effects of the pulsations. Figures 14 and 15 illustrate the effects of poor seeing on the results. The first secondary eclipse (Figure 14) was observed under excellent conditions whereas Figure 15 shows an eclipse observed close to the date of full

moon with poor transparency. The frequency of the dominant pulsation is  $15.23 \pm 0.23$  c/d.

## 4. Conclusions

Our photometric data for the five systems described here indicate that the primary components are the pulsators. The primary eclipses of all the targets show distortions caused by the pulsations of the primary star, indicating that all the systems are inclined to our line-of-sight. The pulsations also show greater amplitude during the primary eclipses caused by the spatial filtering effect (Gamarova *et al.* 2003) when the secondary star blocks some of the primary star's light allowing discrete pulsation zones to be observed independently of others.

The frequencies and amplitudes of the pulsations are typical of those of  $\delta$  Scuti stars. The spectral classifications (Table 2) also indicate that the primaries are in the instability strip of the H-R diagram.

Two types of binaries with pulsating components are recognized. The first type consists of detached systems with no mass exchange, with the pulsator being a typical  $\delta$  Sct star. The second type, oscillating EA systems (oEAs), has been defined by Mkrtichian *et al.* (2004) as eclipsing Algol (EA) binaries with a pulsating,  $\delta$  Sct star. These types of binaries are semi-detached with the primary component undergoing mass accretion from a larger secondary that has filled its Roche lobe. The evolution of the  $\delta$  Sct component in these systems is different from those in the first category.

We are conducting additional photometric studies combined with radial velocity measurements for a better understanding of each of these targets and to determine in which of these categories our targets fit.

## 5. Acknowledgements

Margaret Streamer thanks Dr. Simon Murphy, Sydney Institute for Astronomy, University of Sydney, for his help and advice on the correct use of PERIOD04. Margaret Streamer acknowledges grants from Variable Stars South to purchase software. This research has made use of the International Variable Star Index (VSX) database, operated at AAVSO, Cambridge, Massachusetts, USA.

## References

- Ebbighausen, E. G., and Penegor, G. 1974, *Publ. Astron. Soc. Pacific*, **86**, 203.
- Gamarova, A. Yu., Mkrtichian, D. E., Rodriguez, E., Costa, V.,

and Lopez-Gonzalez, M. J. 2003, in *Interplay of Periodic, Cyclic and Stochastic Variability in Selected Areas of the H-R Diagram*, ed. C. Sterken, ASP Conf. Ser. 292, Astronomical Society of the Pacific, San Francisco, 369.

Giuricin, G., Mardirossian, F., and Mezzetti, M. 1984, *Astrophys. J., Suppl. Ser.*, **54**, 421.

Gray, R. O. 2013, *A Digital Spectral Classification Atlas*, (<http://stellar.phys.appstate.edu/Standards/stdindex.html>); <http://ned.ipac.caltech.edu/level5/Gray/frames.html>).

Hambleton, K. M., et al. 2013, *Mon. Not. Roy. Astron. Soc.*, **434**, 925.

Kholopov, P. N., et al. 1985, *General Catalogue of Variable Stars*, 4th ed., Moscow.

Lenz, P., and Breger, M. 2005, *Commun. Asteroseismology*, **146**, 53.

Liakos, A., and Niarchos, P. 2015, in *Living Together: Planets, Host Stars and Binaries*, ed. S. M. Rucinski, G. Torres, and M. Zejda, ASP Conf. Ser. 496, Astronomical Society of the Pacific, San Francisco, 195.

Mkrtychian, D. E., et al. 2004, *Astron. Astrophys.*, **419**, 1015.

Moriarty, D. J. W., Bohlsen, T., Heathcote, B., Richards, T., and Streamer, M. 2013, *J. Amer. Assoc. Var. Star Obs.*, **41**, 182.

Murphy, S. J. 2015, *Investigating the A-Type Stars Using Kepler Data*, in Springer Theses (<http://link.springer.com/book/10.1007/978-3-319-09417-5>).

Pojmański, G. 1997, *Acta Astron.*, **47**, 467.

Streamer, M., et al. 2015, *J. Amer. Assoc. Var. Star Obs.*, **43**, 67.

Svechnikov, M. A., and Kuznetsova, E. F. 1990, *Approximate Photometric and Absolute Elements of Eclipsing Variable Stars*, A. M. Gorky Univ. of the Urals, Sverdlovsk (<http://cdsarc.u-strasbg.fr/viz-bin/Cat?V/124>).

Thinking Man Software. 1992–2014, DIMENSION 4 software (<http://www.thinkman.com/dimension4/>).

Vanmunster, T. 2013, *Light Curve and Period Analysis Software: PERANSO v.2.50* (<http://www.peranso.com/>).

Watson, C., Henden, A. A., and Price, C. A., 2014, *AAVSO International Variable Star Index VSX* (Watson+, 2006–2014; <http://www.aavso.org/vsx>).

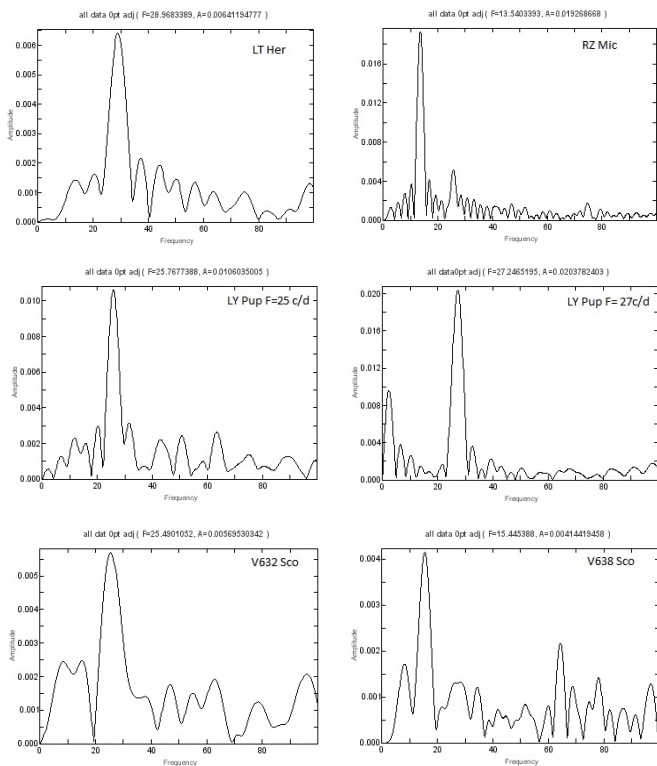


Figure 1. Power spectra for each target.

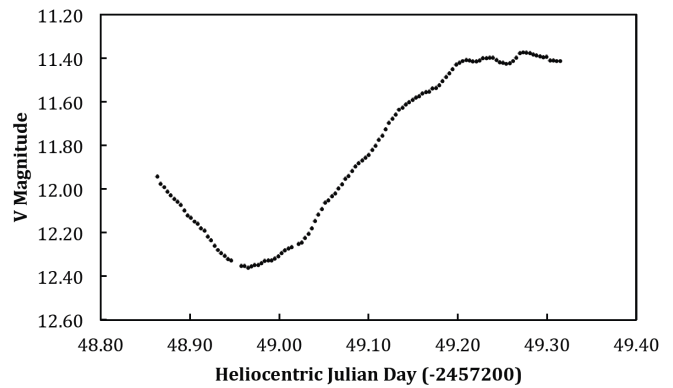


Figure 2. A primary eclipse of RZ Mic.

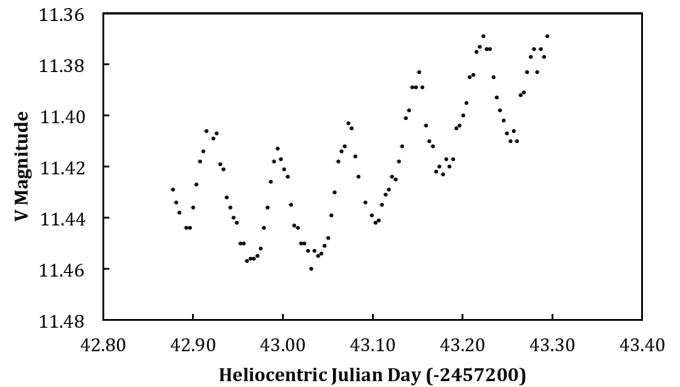


Figure 3. A partial secondary eclipse of RZ Mic.

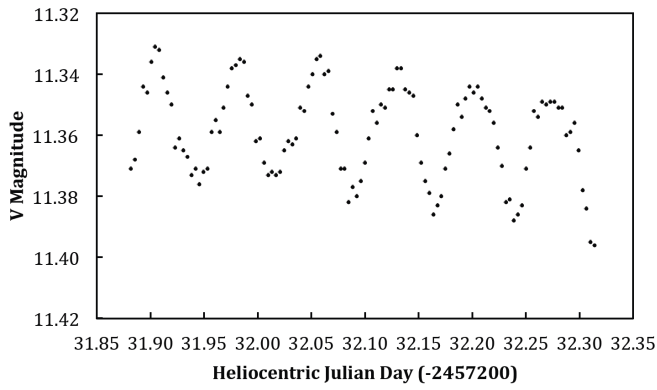


Figure 4. RZ Mic just after quadrature.

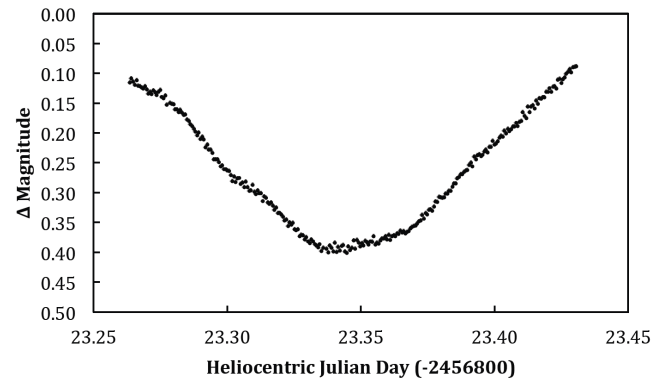


Figure 8. A primary eclipse of LT Her.

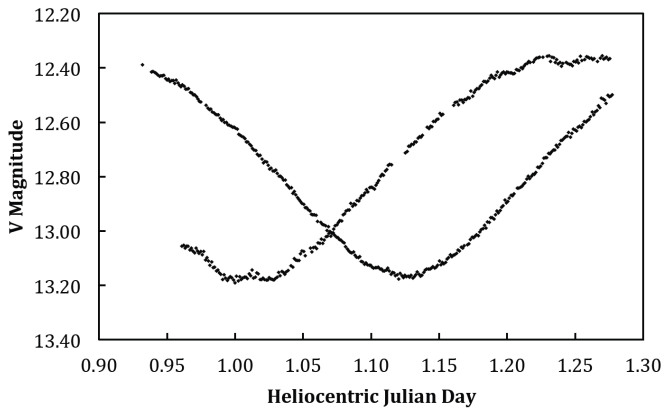


Figure 5. Primary eclipses of LY Pup. The complete eclipse began HJD 2456694.93. The partial eclipse was observed three nights later beginning 2456697.96 .

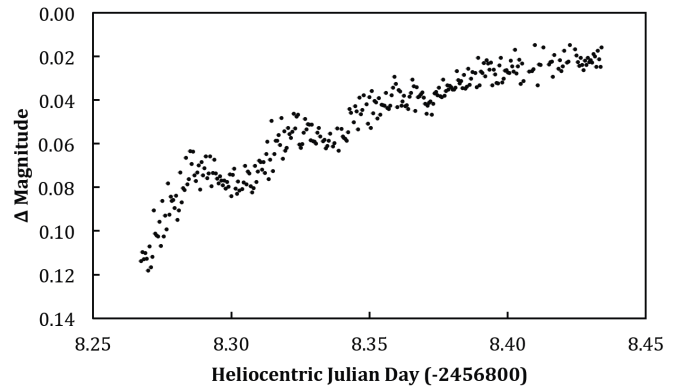


Figure 9. LT Her coming out of primary eclipse.

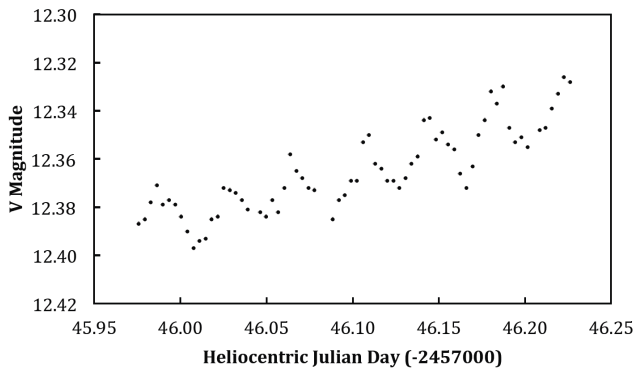


Figure 6. Ascent from a secondary eclipse of LY Pup.

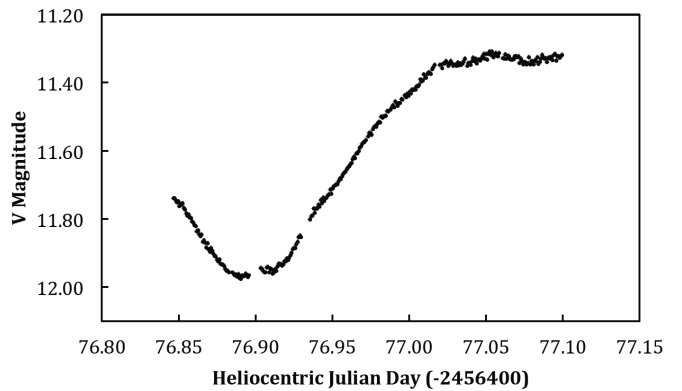


Figure 10. A primary eclipse of V632 Sco.

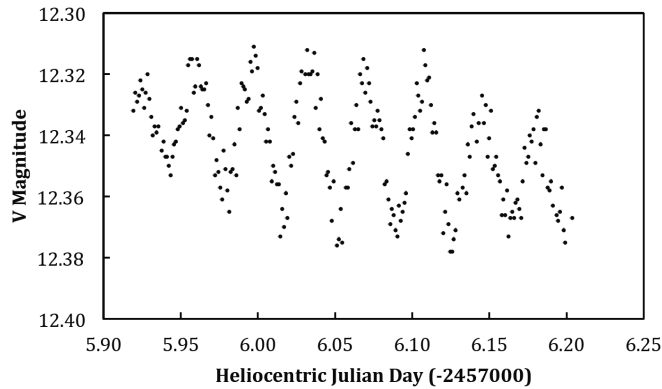


Figure 7. LY Pup out of eclipse.

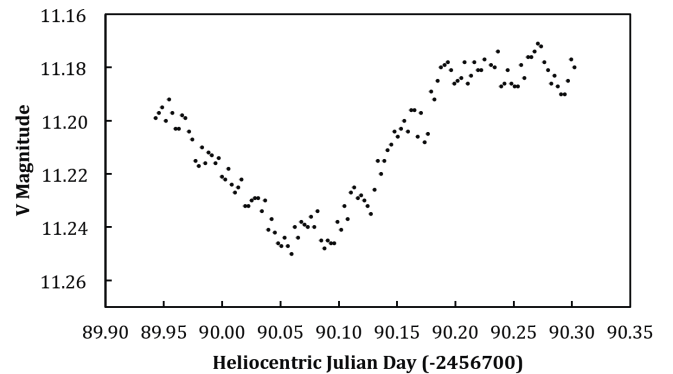


Figure 11. A secondary eclipse of V632 Sco.

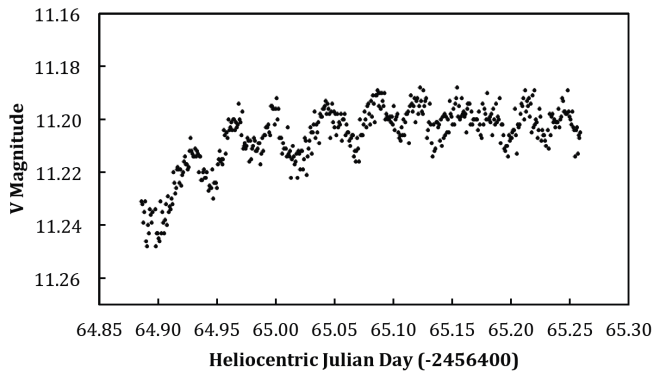


Figure 12. V632 Sco out of eclipse.

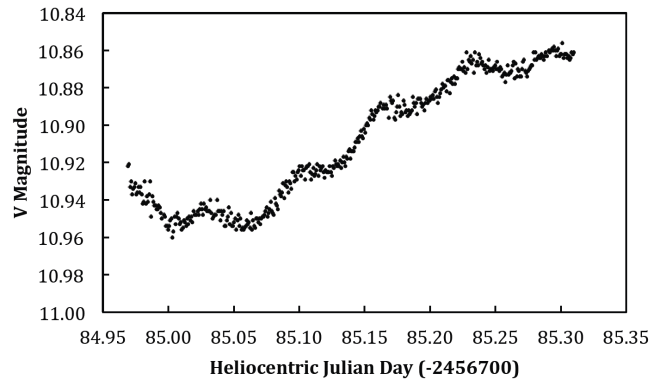


Figure 14. A partial secondary eclipse of V638 Sco.

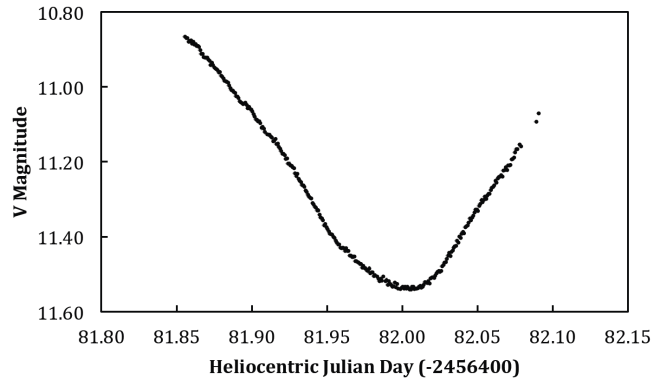


Figure 13. A primary eclipse of V638 Sco.

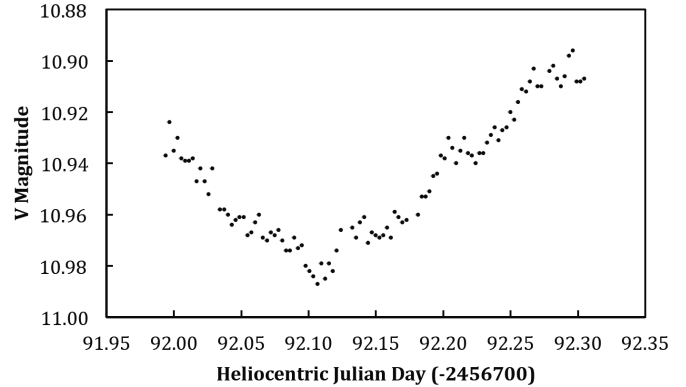


Figure 15. A secondary eclipse of V638 Sco.